Nuclear Engineering and Technology 53 (2021) 61–68

Contents lists available at ScienceDirect

Nuclear Engineering and Technology

journal homepage: www.elsevier.com/locate/net

Original Article

Experimental study on vertically upward steam-water two-phase flow patterns in narrow rectangular channel

Jiancheng Zhou [a], Tianzhou Ye [a], Dalin Zhang [a, *], Gongle Song [a], Rulei Sun [a], Jian Deng [b, **], Wenxi Tian [a], G.H. Su [a], Suizheng Qiu [a]

[a] State Key Laboratory of Multiphase Flow in Power Engineering, Shaanxi Key Lab. of Advanced Nuclear Energy and Technology, School of Nuclear Science and Technology, Xi'an Jiaotong University, Xi'an, 710049, China
[b] Science and Technology on Reactor System Design Technology Laboratory, Nuclear Power Institute of China, Chengdu, China

ARTICLE INFO

Article history:
Received 29 February 2020
Received in revised form
18 May 2020
Accepted 1 June 2020
Available online 2 June 2020

Keywords:
Two-phase flow
Flow patterns
Narrow rectangular channel
Visualization

ABSTRACT

Experiments of vertically upward steam-water two-phase flow have been carried out in single-side heated narrow rectangular channel with a gap of 3 mm. Flow patterns were identified and classified through visualization directly. Slug flow was only observed at 0.2 MPa but replaced by block-bubble flow at 1.0 MPa. Flow pattern maps at the pressure of 0.2 MPa and 1.0 MPa were plotted and the difference was analyzed. The experimental data has been compared with other flow pattern maps and transition criteria. The results show reasonable agreement with Hosler's, while a wide discrepancy is observed when compared with air-water two-phase experimental data. Current criteria developed based on air-water experiments poorly predict bubble-slug flow transition due to the different formation and growth of bubbles. This work is significant for researches on heat transfer, bubble dynamics and flow instability.

1. Introduction

Flat plate fuels are widely used in reactors, aerospace, electronics and some other fields because of its compact structure, relatively low processing requirements, high volume power, low center temperature, high fuel consumption, good safety and some other excellent properties. The flow channel of Flat plate fuels is a typical narrow rectangular channel, and two-phase flow patterns in that channel determine two-phase flow resistance and flow boiling heat transfer characteristics. Flow patterns in narrow rectangular channel are different from those in conventional circular channels due to its unique geometry, so lots of researches have been conducted.

Sadatomi and Saruwatari [1] conducted two-phase flow patterns experiments in vertical rectangular, triangular, circular, and annular channels, and divided flow patterns into bubble flow, slug flow, and annular flow. They presented flow patterns map and concluded that channel geometry has little effect on flow patterns transitions when the hydraulic diameter of channel is greater than 10 mm. Taitel et al. [2] classified the flow patterns into bubble flow, slug flow, churn flow and annular flow in the circular tube channel, which is the traditional classification on flow regimes, and gave the corresponding flow patterns transition criteria. Mishima and Ishii [3] gave the same classification on flow patterns, but proposed new transition criteria. The results show that the criteria for the transition from bubble flow to slug flow and from churn flow to annular flow are in good agreement with experiment data, but the transition from slug flow to churn flow varies widely. This may be attributed to the difference in the proposed basic mechanism of the slug-to-churn flow transition. Xu [4] found the flow characteristics in narrow rectangular channel with the gap of 0.6 mm and 1.0 mm were not much different from those found in traditional channels, but bubbly flow was replaced by cap-bubbly flow in 0.3 mm width channel. He thought bubbly flow is suppressed in such a channel with a thin gap, and small isolated bubbles are squeezed to be coalesced with each other, causing the coalescence of small bubbles to form cap-bubbly flow. Xu [5] improved the distribution parameter of transition criteria in Mishima and Ishii [3], and the revised transition criteria are in good agreement with the experimental result (1.07 mm) in Mishima et al. [6], but the transition is slightly

* Corresponding author.
** Corresponding author.
E-mail addresses: 2872109519@qq.com (J. Zhou), 729832036@qq.com (T. Ye), dlzhang@mail.xjtu.edu.cn (D. Zhang), 834199675@qq.com (G. Song), 1091159125@qq.com (R. Sun), dengjian_npic@163.com (J. Deng).

https://doi.org/10.1016/j.net.2020.06.003

later than that in Wilmarth and Ishii [7]. Churn flow never appeared in Mishima et al. [6] but was found in Xu [5], which may be caused by the confusions between slug flow and churn flow, or churn flow and annular flow. Hibiki and Mishima [8] proposed flow patterns transition criteria for vertical upward flow in narrow rectangular channels based on the same principles of Mishima and Ishii [3], but the difference is that bubbly flow in narrow rectangular channel can be approximated as circles on two-dimensional plane unlike in round tubes. The criteria are satisfactory and coincide well with the results of Wilmarth and Ishii [7] and Mishima et al. [6], but deviated from Xu [5] largely. The reason may be the inconsistent standards for flow patterns identification, which is heavily dependent on the individual observer. Friction pressure drop, flow patterns, and void fraction characteristics of air-water two-phase flow at different angles and flow directions were studied in narrow rectangular channels with gaps of 0.778 mm and 1.465 mm in Ali et al. [9]. Those were found to be similar for all orientations except for horizontal flow, and the effect of the gap width was small. Chalgeri and Jeong [10] carried out researches on vertically upward and downward air-water two-phase flow patterns [11] in a narrow rectangular channel with a gap of 2.35 mm. They found flow patterns in upward flow were similar to traditional flow regime and the transition had the same trend with the result of Wilmarth and Ishii [7]. But in downward flow, flow patterns are divided into bubbly flow, large-bubbly flow, cap-bubbly flow, slug flow, churn turbulent flow, falling film flow, annular flow, and one undefined. Also, there are no satisfactory criteria for downward flow.

Researches were almost conducted on air-water two-phase flow, while little performed on steam-water two-phase flow regimes under heating conditions. Hosler [12] studied steam-water two-phase flow patterns in vertical narrow rectangular channel at heating condition with the pressure from 1 MPa to 9.7 MPa, and bubbly flow, slug flow and annular flow were observed. Flow regime map shows that the transition would become earlier with the pressure increases. A photographic study about flow patterns for flow boiling of water at single-side heated in a vertical narrow rectangular channel have been carried out in Wang et al. [13]. Not only the flow patterns are divided into dispersed bubbly, coalesced bubbly, churn flow, and annular flow, but also the transition criteria are slightly different from those in conventional flow regimes. These significant deviations may be due to the different bubble forms and distributions in heating conditions. In the field of electronic heat dissipation, there are many literatures (Revellin and Thome [14], Arcanjo et al. [15], Fu et al. [16], Li et al. [17]) focusing on steam-water two-phase flow patterns in narrow channels. After all, it is different from the conventional narrow rectangular channel due to the great influence of surface tension and domestic inertia force on the bubbles. There are also some numerical research [18,19] on flow characteristics in narrow rectangular channel, but they lack experimental verification.

As stated above, researches on two-phase flow patterns under heating conditions in narrow rectangular channel are very limited. This work investigates vertically upward steam-water two-phase flow regime under heating conditions at different pressure through single side visualization in narrow rectangular channel with a large aspect ratio. The flow patterns characteristics and transitions were conducted visually and compared with others'.

2. Experimental method

2.1. Experimental apparatus

The experimental loop is shown in Fig. 1, and working fluid is deionized water treated with anion and cation exchanger. The test loop is divided into two parts: the primary experimental loop with test section and cooling loop. The primary experimental loop is mainly composed of high-pressure plunger pump, regenerator, preheating section, test section, condenser, water tank, etc. The cooling loop, mainly cooling the flow water in main experimental loop, is mainly composed of condenser, cooling water tank, condensation pump, cooling tower, etc.

The flowing water is diverted into two pipes by high-pressure plunger pump after passing the valve and filter from water tank. One is the bypass system designed to adjust the flow and pressure; the other is the primary experimental loop, in which the working fluid enters the high efficient regenerative double-pipe heat exchanger after passing the regulating valve and the flow meter, absorbing the heat from the working fluid flowing out from the test section. And then, the working fluid enters the preheating section, which can heat the water to the required temperature for the inlet of test section. Water would be heated to boiling in test section, where two-phase flow is observed visually, and condensed by heat exchanger and condenser. Lastly, it returns to the water tank, and a cycle is completed.

2.2. Test section

The schematic diagram of the test section is shown in Fig. 2. It mainly includes narrow rectangular flow channel, heating plate, conductive copper column, inlet and outlet, visual window, supporting structure and measurement structure etc. The test section is entirely covered with thermal insulation cotton except visual window to reduce heat dissipation.

A rectangular groove is milled on the stainless steel plate, and a rectangular stainless steel heating plate is embedded. The heating plate and the stainless steel pressure shell are insulated by insulating ceramic. The narrow-side insulating ceramic fixs the width of the flow channel, and the gap of channel is determined by mating between the narrow-side insulating ceramic and the wide-side insulating ceramic. Water would be heated to boiling at 1 MPa, so visual window that can withstand high temperature and high pressure becomes the key component of this test section. There is a large square cavity between the inner glass and the outer glass in this test section storing still water. The square cavity is interconnected with the rectangular channel at outlet, but sealed at inlet, so the pressure in them are the same and the water in the cavity does not flow. The inner glass can withstand high temperature fluctuations and the outer glass can withstand high pressure. This structure design prevents the rapid cooling and heating of the fluid in the rectangular channel from causing the outer glass to crack.

In this experiment, the water is directly heated into two-phase flow boiling through a heating plate. The heating plate, whose electric resistance is very small, is connected with low voltage and high current DC power supply, and would generate a lot of heat. DC power supply can achieve uniform heating, and has no charge accumulation. The heating plate has 590 mm length and 70 mm width, and the gap of the rectangular channel is 3 mm. Certain length is reserved before and after the effective heating section as a transition section to eliminate the inlet and outlet effects and ensure that the fluid fully develops in the vertical narrow rectangular channel.

Preset flow rate and pressure are obtained by adjusting the pump and the valve, and inlet temperature required for test condition is obtained by adjust the power of preheating section. When bubbles appear in the channel through slowly increasing the heating power of test section, and image data and corresponding parameters would be recorded, especially focusing on visualization image and corresponding parameters when flow patterns transition occurs at the end of the plate. Other conditions can be carried out by changing mass flow rate and repeating the above steps.

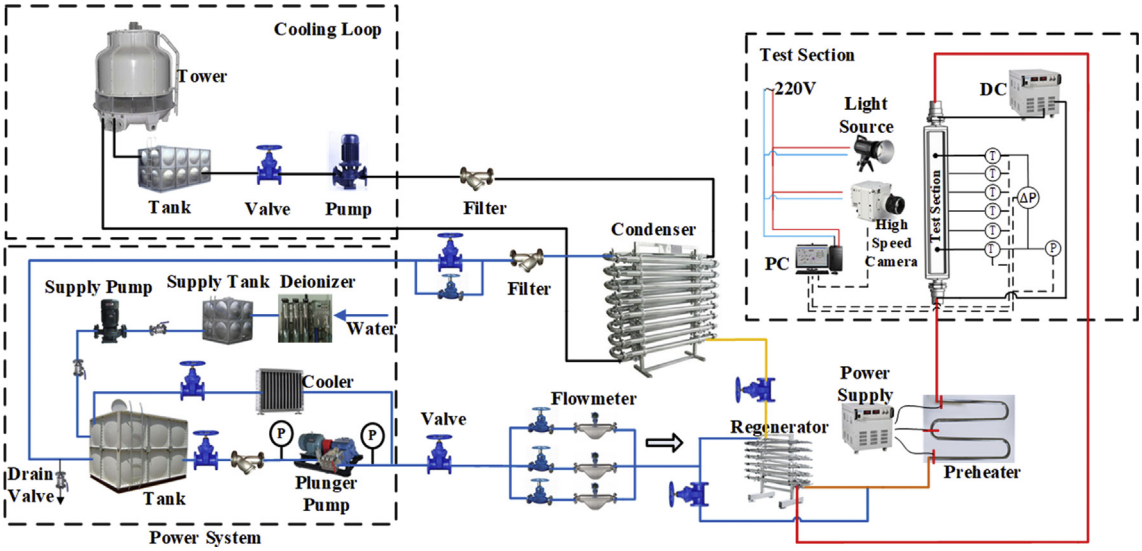

Fig. 1. Schematic diagram of experimental loop.

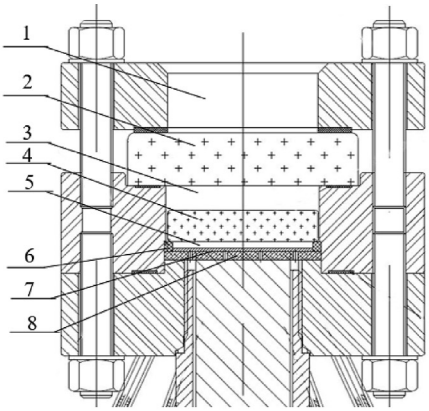

1——Visualization Windows 2——Outer Glass 3——Buffer Cavity 4——Inner Glass 5——Narrow Rectangular Channel 6——Narrow-side Insulating Ceramic 7——Heating Plate 8——Wide-side Insulating Ceramic

Fig. 2. Schematic diagram of test section.

2.3. Measurement and data acquisition

K-type armored thermocouples are arranged in the channel before and after the effective heating section to measure the temperature of inlet and outlet fluids, and thermocouples on the back of the heating plate are evenly spaced to measure the wall temperature. At the same time, pressure holes are set at the inlet and outlet to measure the pressure and pressure difference. The heating power of heating plate is obtained by measuring the voltage and current. Coriolis mass flow meter produced by EMERSON is installed before preheating section. All signals are obtained through processing by NI data acquisition system, and its uncertainty is 0.02%. Flow patterns image is acquired by Phantom VEO 640 high-speed digital camera. In this experiment, flow patterns in the channel are recorded at a frame rate of 500 frames/s and image data is stored in PC at the same time.

The uncertainty of experimental measured results mainly comes from the uncertainty of measuring instrument and the uncertainty of data acquisition system. Assuming that the measuring error of instrument obeys a uniform distribution, the standard uncertainty of any parameter measured can be estimated by the following formula [20]. The uncertainties of all measuring parameters in this experiment are shown in Table 1.

$$\frac{\Delta R}{R}=\sqrt{\left(\frac{\Delta x_1}{x_1}\right)^2+\left(\frac{\Delta x_2}{x_2}\right)^2+\ldots+\left(\frac{\Delta x_n}{x_n}\right)^2}$$

Table 1
Experimental parameter ranges.

Item	Parameter range	Max uncertainty
Mass flux(kg/h)	0–750	0.201%
Pressure(Mpa)	0–1.0	0.251%
Pressure difference(kpa)	−6.2–6.2	0.251%
Temperature(°C)	60–180	1–2 °C
Heating current(A)	800–3000	0.5%
Heating voltage(V)	5–20	0.1%
Heat flux(kw/m^2)	200–1000	0.52%

3. Results and discussions

The flow pattern maps at 0.2 MPa and 1 MPa have been investigated respectively. As can be seen in Fig. 3 and Fig. 4, bubble flow, slug flow and churn flow are identified at 0.2 MPa, while slug flow is replaced by block bubble flow at 1 MPa, shown in Fig. 4(b). During the period of annular flow, the flow channel is close to dryout, and the liquid phase is just in the form of droplet in the vapor phase. At this time, [21,22] CHF would be triggered easily and cause the heating plate to burn out. Therefore, the study of annular flow has not been carried out for the time being.

3.1. Flow patterns at 0.2 MPa

3.1.1. Bubble flow

In the middle of the mainstream, small bubbles are densely distributed, but the mainstream is subcooled. Small bubbles are attached to the heating wall and slide forward. If bubbles leave the wall and enter the mainstream, they will annihilate. At the two narrow-sides, large bubbles are generated, but restricted by the gap of channel, and the bubbles are compressed into flat shape. The large bubbles can only be observed at narrow side, revealing heat transfer deteriorates or weak flow appears. Especially, when the large flat bubbles are dragged to center, they would be cooled down. As a result, small bubbles observed at center display the same size. While large flat bubble at narrow-side grow faster than the rate of annihilate, the bubbles would continuously laterally grow to form Taylor bubbles. At this time, flow patterns transform from bubble flow into slug flow.

3.1.2. Slug flow

When the heat flux further increases in late period of bubble flow, bubbles at narrow-side of channel begin to coalesce and grow, the growth rate of bubbles sharply increases, and the small bubbles attached to the heating wall in central area are engulfed. Finally, a large long flatten bubble is formed, with a semi-circular front and a nearly flat tail, in the middle of which a small amount of droplets diffuse. Unlike Taylor bubble in air-water two-phase flow, those bubbles are intermittently generated at narrow-sides, and the starting positions are randomly distributed. In the late period of slug flow, large long flat bubbles are generated at both narrow-sides intermittently, sometimes simultaneously. Bubbles would squeeze each other, forming a long liquid film in the middle of the flow channel.

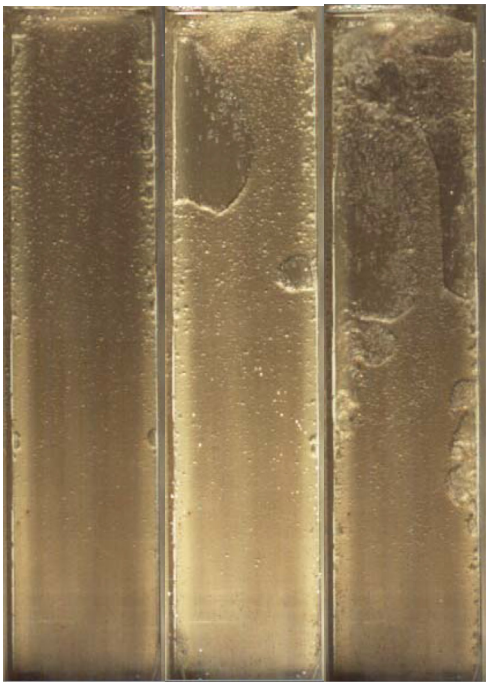

(a)bubble flow (b) slug flow (c)churn flow

Fig. 3. Flow patterns at 0.2Mpa.

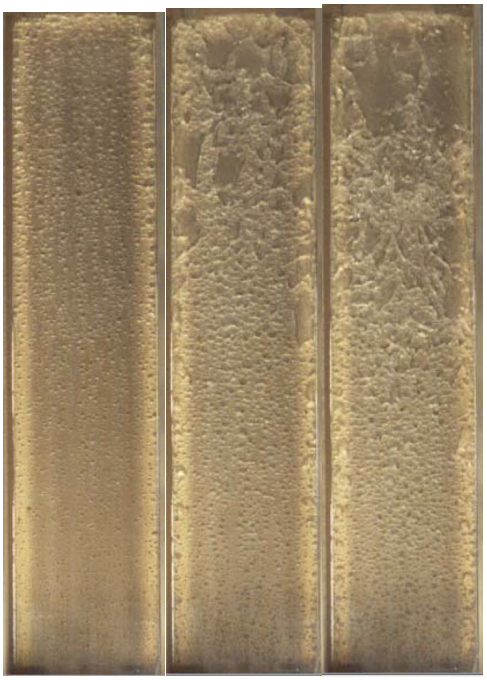

(a)bubble flow (b)block bubble flow(c)churn flow

Fig. 4. Flow patterns at 1.0Mpa.

3.1.3. Churn flow

In the late period of slug flow, the nose of long flatten bubbles break up due to high heat flux and turbulence, and flow patterns transform into churn flow. The long flat bubbles produced at two narrow-sides squeeze each other, and the long liquid film swings left and right and hits narrow-sides, slapping abundant droplets and forming large wave. After that hitting, flow stagnation and even flow reversal would occur, which is more obvious at low flow rate. There are still endless small droplets moving forward in the long flat bubbles, whose velocities are exceedingly larger than bubbles'.

3.2. Flow patterns at 1 MPa

3.2.1. Bubble flow

In the center of the channel, small bubbles are densely dispersed, but the bubbles are larger and more densely distributed than those observed at 0.2 MPa. Confined by height of the gap, the bubbles are flattened in the direction of height after growing, and approximately observed as circles at two-dimensional plane. The sizes of bubbles at the same cross section in center are basically the same. Near the two narrow-sides, bubbles grow faster than the center's and the size is larger. The diameter of bubbles exceeds the gap of channel, so bubbles slide forward against the front and rear walls. During the flow, the shape of bubbles are constantly slightly changing with no fixed shape, but overall they are still round. In this

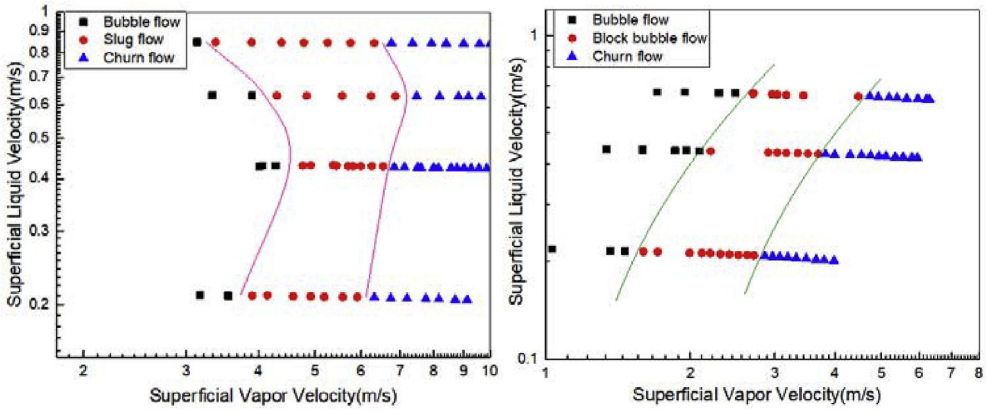

Fig. 5. Flow pattern maps at 0.2Mpa(a) and 1.0Mpa(b).

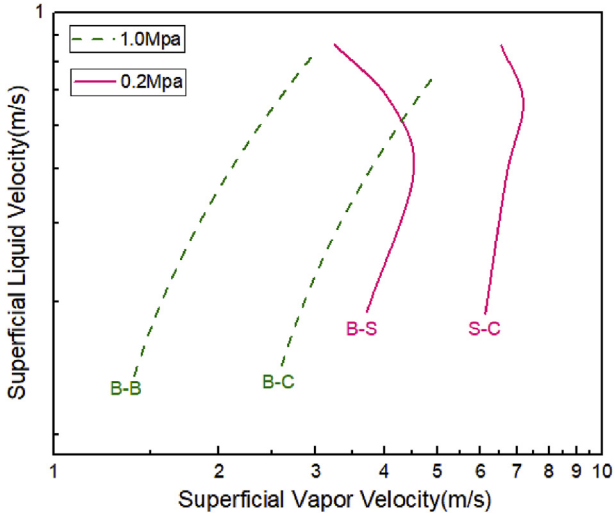

Fig. 6. Pressure effects on flow pattern transitions.

process, the growth of bubbles mainly depends on the evaporation of liquid film at the heating wall and its devouring small bubbles attached to the heating wall, however there is no coalescence between the same size bubbles at the same cross section.

3.2.2. *Block bubble flow*

The deformed bubbles begin to coalesce and bubbles grow quickly, and they become flat block-like bubbles. The bubbles are seriously deformed and extrude each other. In addition to the impact of heat flux and flow turbulence, the boundary of flat block-like bubbles becomes extremely irregular, and distorts extremely, and the block-like bubbles have no fixed shape during the upward flow. In Wang et al. [13], this flow pattern is called coalesced bubbly flow, but block bubble flow maybe more in consistent with its characteristics due to bubbles embed mutually like blocks.

In this flow patterns, the growth of bubbles in this process is mainly depended on coalescence between bubbles, and the growth is limited to the width and length of the channel. The sizes of block-like bubbles vary from each other, and appear early at narrow-side, due to the poor heat transfer coefficient and weak flow. Bubbles deform and distort severely, especially at high heat flux corresponding to high flow rate. In the late stage of block bubble flow, block-like bubbles begin to coalesce and void fraction further increases.

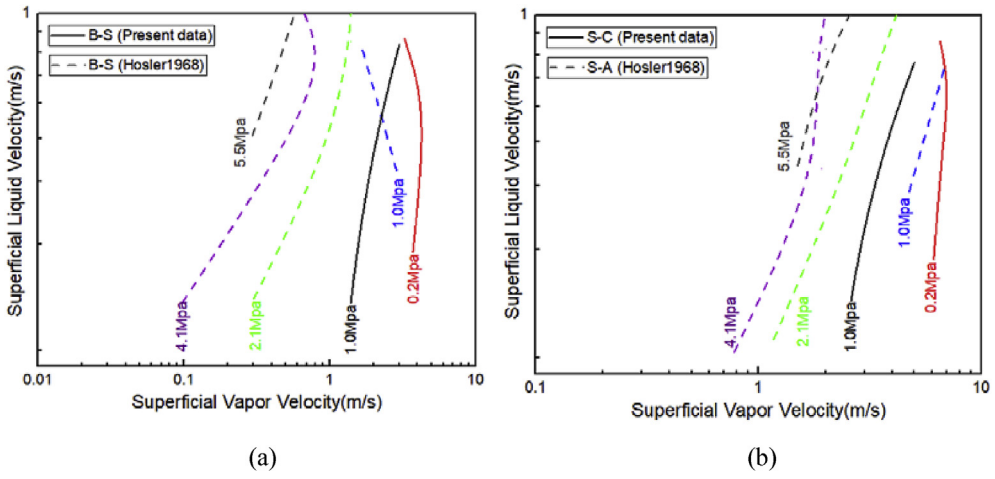

Fig. 7. Flow pattern maps in heated channel compared with Hosler [12] data.

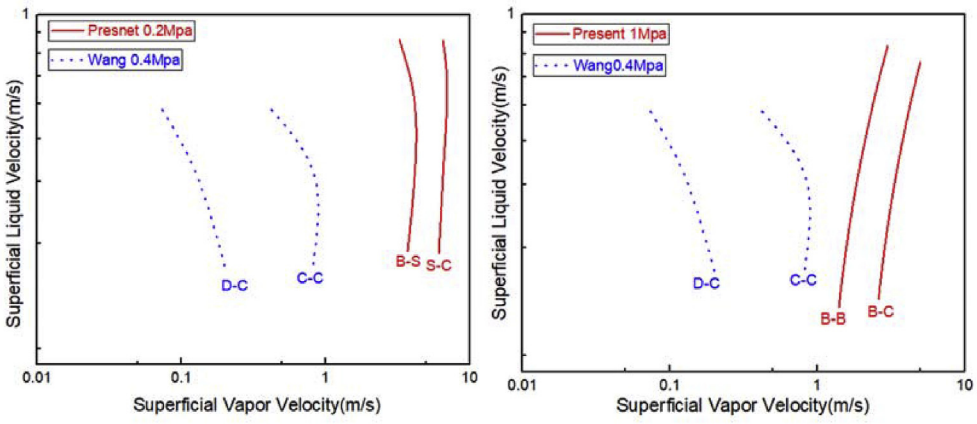

Fig. 8. Flow pattern maps in heated channel compared with Wang et al. [13] data.

3.2.3. Churn flow

Flatten bubbles would be broken up by wall shearing force, flow turbulence, and heat flux when bubbles grow up to a certain critical size. Steam-vapor nearly fills the entire cross section. As a result of bubbles breaking up, liquid phases collide with each other and produce many waves dispersed in vapor phases. The interface between vapor-phase and liquid-phase is chaotic and indistinguishable.

In this flow pattern, there are no shaped bubbles, and the channel is dominated by vapor phase. The liquid phase is flaky or filament-like dispersed in the vapor phase and sometimes liquid films are interconnected to form a network structure. Affected by bubbles breaking up, the liquid phase flow will stagnate or even reverse partly. Steam-water two-phase turbulence is very serious.

3.3. Flow pattern maps

Flow pattern transitions are affected by many factors, such as fluid properties, inlet subcooling and the surface roughness of the heating walls, etc. Actually, the observed flow patterns boundaries are not distinctive lines, but a wide transition region where the transition occurs gradually. For representation, the transition zones are depicted as distinct lines. And they merely represent the general trends, but not the precise location [10]. Generally, flow pattern maps are presented with superficial vapor velocity($J_v = Gx/\rho_v$)as the abscissa and superficial liquid velocity($J_l = G(1-x)/\rho_l$)as the ordinate. According to the definition of vapor quality at thermal equilibrium:

$$x_e = \left(h_{in} + Q \Big/ G - h_f\right) \Big/ h_{fg}$$

The real vapor quality should be revised by Levy [23] model when the outlet is at subcooled boiling:

$$x = x_e - x_{eB} \exp\left(\frac{x_e}{x_{eB}} - 1\right)$$

Where x_{eB} is the vapor quality at thermal equilibrium corresponding to the bubble departure point, calculated according to Bowring model.

The flow patterns at 0.2 MPa and 1 MPa are shown in Fig. 5. Fig. 6 shows the pressure effect on flow regime transitions. Both the bubbly–slug(block bubble) flow transition and slug(block bubble)-churn flow transition occur earlier with pressure increasing. This may be due to the fact that the vapor density is higher while the system pressure increases, and superficial vapor velocity decreases correspondingly. As a result, the flow patterns transition occurs earlier. In addition, bubble-slug flow transition requires a large range of bubbles to coalesce to form a long flatten bubble, but bubble-block bubble flow transition only need bubbles to coalesce in small region to form relatively small block-like bubbles, which requires lower vapor quality and superficial vapor velocity. Similarly, the condition for slug-churn flow is rigorous than block bubble-churn flow. The former needs the nose of long flatten bubbles to break up while the latter just needs the block-like bubbles to coalesce or break up, which is relatively easier.

Similar phenomena could be found in Hosler's [12] data, although he didn't find churn flow. As shown in Fig. 7, comparision between present flow pattrens transition and Hosler's [12] has been conducted. The present transition at 0.2 MPa is higher than those given by Hosler [12] due to the effect of pressure. And the present transition at 1 MPa shows great agreement with Hosler [12],especially at the same pressure, though there is a litter deviation which can be accounted by different geometric conditions.

Fig. 8 shows comparison with the transition given by Wang et al. [13] for steam-water two-phase vertically upward flow in 3 mm gap narrow rectangular channel at 0.4 MPa, whose heating plate are 470 mm length and 40 mm width. His result is significant for our experiment because the geometry of his test section and the thermos-hydraulic parameters of his experiment are quite similar to this study. As can be seen in the figure, both of the transitions in Wang et al. [13] shifts significantly towards left. The reason may be the great difference in heat flux. The effective heating area of Wang et al. [13] is less than half of present experiment's and additionally inlet subcooling is 80 °C, while it is 60 °C in present experiment. As a result, the heat flux in Wang et al. [13] is much larger at the same vapor quality, corresponding to severer disturbance and deformation on bubbles. Besides, the smaller width of channel leads to more serious accumulation of bubbles. All of those factors cause the easier coalescence and transitions occur more rapidly.

Comparison of air-water two-phase flow experimental data in adiabatic channel and flow transition criteria model has been conducted. The flow regime transition lines for the vertical upward flow experiment of Xu [4] through a narrow rectangular test section with the gap width of 0.6 mm and 1.0 mm are compared with the present flow regime maps in Fig. 9. All of the transitions shift right especially at 0.2 MPa. In adiabatic channel, the superficial velocities of vapor and liquid phases along the path keep the same. As long as the adjacent bubbles break through surface tension from each

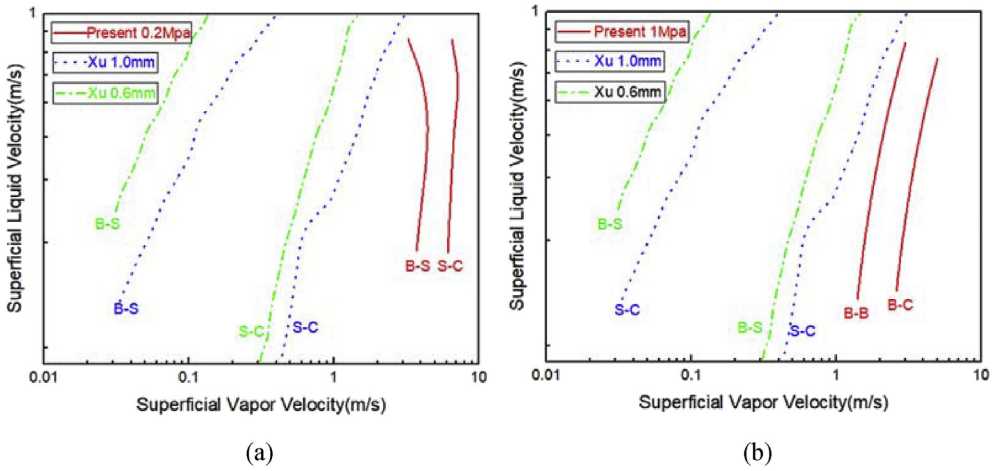

Fig. 9. Flow pattern maps in heated channel compared with Xu [4] data.

other, they would coalesce to form Tayler bubbles, which will cause the flow pattern transition. However, bubbles continually increase along the heating channel and the macro-parameters such as vapor quality and void fraction are not a constant value. Bubbles are generated by the evaporation of the heated liquid phase. With the continual heat flux, bubbles expand and accelerate downstream fluids, which is equivalent to pushing the downstream bubbles away, leading to difficulties of bubbles coalescence. As a result, the flow patterns transitions delay. This phenomenon can also explain why the slug-churn transition in this experiment is later than that in Xu's [4] experiment. In heating channel, a higher void fraction is required to achieve the flow patterns transiton. Only with bubbles growing to certain critical extent and reducing the liquid phase barrier between them, can transitions occur.

Fig. 10 shows a comparison of flow pattern transition criteria developed by Hibiki and Mishima [8] for a vertically upward flow in narrow rectangular channel with the present experimental data. As can be seen in the figure, the present data agrees well with the block bubble-churn flow transition at 1 MPa and shift right a little with the slug-churn flow transition at 0.2 MPa. However, the bubble-slug transition and bubble-block bubble transition shifts significantly towards the right and many of bubble flow regions lie outside the modeled region.

The transition criteria from bubble flow to slug flow is based on the improvement of Mishima and Ishii's [3] model.The possibility of collisions and coalescence is considered to increase significantly if the maximum possible distance between two bubbles becomes less than a projected diameter of a flat bubble of $2R_b$. The bubbly flow to slug flow transition is considered to occur under this condition, namely void fraction α varying from 0.2 to 0.3 [8]. Nevertheless, bubbles don't coalesce even when the distance between bubbles is less than a projected radius in the present heating channel. The void fraction in heating channel is much higher than that in adiabatic channel due to the different generation method of bubbles, and the corresponding transition occurs significantly later.

4. Conclusions

In present study, experiment of vertically upward steam-water two-phase flow in heated narrow rectangular channel has been carried out and flow patterns maps at 0.2 MPa and 1.0 MPa have been plotted based on the measured data. Three different flow patterns, namely bubble flow, slug flow, and churn flow were identified at 0.2 MPa while slug flow did not appear and were replaced by block-bubble flow at 1.0 MPa. The study of annular flow, for which CHF maybe triggered easily, has not been carried out yet for the protection of heating plate. Flow patterns were identified and classified with direct visualization analysis.

Flow pattern maps at 0.2 MPa and 1.0 MPa were compared with other's experimental results and transition criteria. Both the

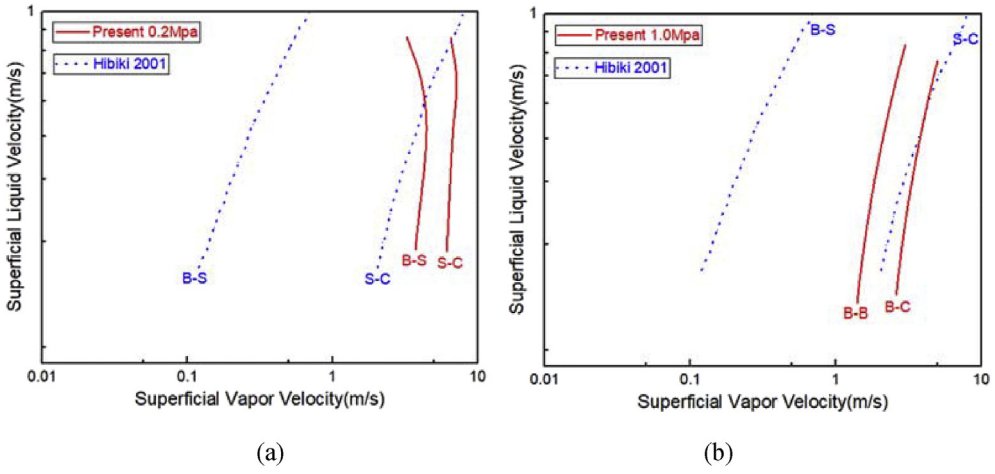

Fig. 10. Flow pattern maps in heated channel compared with transition criteria developed by Hibiki and Mishima[8].

present result and Hosler's [12] data conclude that the flow pattern transitions shift left with pressure increasing, and the transition line at 1 MPa reasonably conforms to the present data. Comparison of experimental data with Wang et al.'s [13] shows heat flux has large effect on transition, due to the disturbance and deformation of bubbles. Experimental result on air-water two-phase flow given by Xu [4] does not fit well with present data, because of the different bubbles generation methods and gap widths of channel. Transition criteria from slug flow to churn flow developed by Hibiki and Mishima [8] in narrow rectangular channels show great agreement with present data, while bubble-slug transition criteria poorly predict it owing to the observed discrepancy of void fraction. With comparisons stated above, it should be noted that further experiments with various thermal parameters and geometric parameters are needed to develop new flow pattern transition criteria which are suitable for vertically steam-water two-phase flow at heating conditions in narrow rectangular channel.

Declaration of competing interest

The authors declare that they have no known competing financial interests or personal relationships that could have appeared to influence the work reported in this paper.

Acknowledgements

The authors gratefully acknowledge the supports from Natural Science Foundation of China (Grant No. 11675127) and K. C. Wong Education Foundation.

Appendix A. Supplementary data

Supplementary data to this article can be found online at https://doi.org/10.1016/j.net.2020.06.003.

References

[1] M. Sadatomi, Y. Sato, S. Saruwatari, Two-phase flow in vertical noncircular channels, Int. J. Multiphas. Flow 8 (6) (1982) 641–655.
[2] Y. Taitel, D. Bornea, A.E. Dukler, Modelling flow pattern transitions for steady upward gas-liquid flow in vertical tubes, AIChE J. 26 (3) (1980) 345–354.
[3] M. Kaichiro, M. Ishii, Flow regime transition criteria for upward two-phase flow in vertical tubes, Int. J. Heat Mass Tran. 27 (5) (1984) 723–737.
[4] J. Xu, Experimental study on gas–liquid two-phase flow regimes in rectangular channels with mini gaps, Int. J. Heat Fluid Flow 20 (4) (1999) 422–428.
[5] J.L. Xu, P. Cheng, T.S. Zhao, Gas–liquid two-phase flow regimes in rectangular channels with mini/micro gaps, Int. J. Multiphas. Flow 25 (3) (1999) 411–432.
[6] K. Mishima, T. Hibiki, H. Nishihara, Some characteristics of gas-liquid flow in narrow rectangular ducts, Int. J. Multiphas. Flow 19 (1) (1993) 115–124.
[7] T. Wilmarth, M. Ishii, Two-phase flow regimes in narrow rectangular vertical and horizontal channels, Int. J. Heat Mass Tran. 37 (12) (1994) 1749–1758.
[8] T. Hibiki, K. Mishima, Flow regime transition criteria for upward two-phase flow in vertical narrow rectangular channels, Nucl. Eng. Des. 203 (2–3) (2001) 117–131.
[9] M.I. Ali, M. Sadatomi, M. Kawaji, Adiabatic two-phase flow in narrow channels between two flat plates, Can. J. Chem. Eng. 71 (5) (1993) 657–666.
[10] V.S. Chalgeri, J.H. Jeong, Flow patterns of vertically upward and downward air-water two-phase flow in a narrow rectangular channel, Int. J. Heat Mass Tran. 128 (2019) 934–953.
[11] T.H. Kim, V.S. Chalgeri, W. Yoon, et al., Visual observations of flow patterns in downward air-water two-phase flows in a vertical narrow rectangular channel, Ann. Nucl. Energy 114 (2018) 384–394.
[12] E.R. Hosler, FLOW PATTERNS IN HIGH PRESSURE TWO-PHASE (STEAM–WATER) FLOW WITH HEAT ADDITION[R], Bettis Atomic Power Lab., Pittsburgh, Pa., 1967.
[13] J. Wang, Y. Huang, Y. Wang, Photographic study on two-phase flow patterns of water in a single-side heated narrow rectangular channel, J. Eng. Gas Turbines Power 133 (5) (2011).
[14] R. Revellin, J.R. Thome, A new type of diabatic flow pattern map for boiling heat transfer in microchannels, J. Micromech. Microeng. 17 (4) (2007) 788.
[15] A.A. Arcanjo, C.B. Tibiriçá, G. Ribatski, Evaluation of flow patterns and elongated bubble characteristics during the flow boiling of halocarbon refrigerants in a micro-scale channel, Exp. Therm. Fluid Sci. 34 (6) (2010) 766–775.
[16] B.R. Fu, P.H. Lin, M.S. Tsou, et al., Flow pattern maps and transition criteria for flow boiling of binary mixtures in a diverging microchannel, Int. J. Heat Mass Tran. 55 (5–6) (2012) 1754–1763.
[17] X. Li, L. Jia, C. Dang, et al., Visualization of R134a flow boiling in microchannels to establish a novel bubbly-slug flow transition criterion, Exp. Therm. Fluid Sci. 91 (2018) 230–244.
[18] Tangtao Feng, Mingjun Wang, Ping Song, Luguo Liu, Wenxi Tian, G.H. Su, Suizheng Qiu, Numerical research on thermal mixing characteristics in a 45-degree T-junction for two-phase stratified flow during the emergency core cooling safety injection, Prog. Nucl. Energy 114 (2019) 91–104.
[19] Linfeng Li, Di Fang, Dalin Zhang, Mingjun Wang, Wenxi Tian, Guanghui Su, Suizheng Qiu, Flow and heat transfer characteristics in plate-type fuel channels after formation of blisters on fuel elements, Ann. Nucl. Energy 134 (2019) 284–298.
[20] R. Sun, G. Song, D. Zhang, et al., Experimental study of single-phase flow and heat transfer in rectangular channels under uniform and non-uniform heating, Exp. Therm. Fluid Sci. (2020) 110055.
[21] GL Song, Liang Y , Sun R , et al., A critical heat flux model for unilateral heating rectangular narrow channel, Annals of Nuclear Energy (2020), https://doi.org/10.1016/j.anucene.2020.107419.
[22] GL Song, Liang Y, Sun R , et al, A Dryout mechanism model for rectangular narrow channels at high pressure conditions, Nuclear Engineering and Technology (2020), https://doi.org/10.1016/j.net.2020.03.018.
[23] S. Levy, Forced convection subcooled boiling: prediction OF vapor volumetric fraction, Int. J. Heat Mass Tran. 10 (7) (1967) 951–965.